COMPARISON OF ONE-DIMENSIONAL AND TWO-DIMENSIONAL MODELING OF CATALYTIC NAPHTHA REFORMING PROCESS IN AXIAL FLOW SPHERICAL PACKED-BED REACTOR

S. Zaree, M. Jafari, D. Iranshahi, M.R. Rahimpour*

School of Chemical and Petroleum Engineering, Department of Chemical Engineering, Shiraz University, Shiraz, Iran

*Corresponding author: Tel.: +98 711 2303071 fax: +98 711 6287294 *E-mail address:* rahimpor@shirazu.ac.ir

ABSTRACT

In the present research, the differences between one-dimensional and two-dimensional modeling of catalytic naphtha reforming process in axial flow spherical packed-bed reactor (AF-SPBR) have been investigated. After writing the mass, energy and momentum balances, thermodynamic and kinetic equations, and auxiliary relations, the reactor has been modeled with Computational Fluid Dynamics (CFD) software. In this modeling, the velocity, temperature, and concentration distribution are considered in both axial and radial directions. The velocity profile is pictured to illustrate the radial and axial movement of the fluid thorough the packed-bed of the spherical reactor. In addition, the differences between temperature and concentration distribution of one-dimensional and two-dimensional modeling through the radius and the length of the reactor are investigated. The effect of the entrance velocity on the output concentration of naphthene and aromatic in one-dimensional and two-dimensional modeling is also presented.

NOMENCLATURE

a	catalyst activity, -
Ac	cross-section area of reactor, m^2
c	concentration, kmol m^{-3}
cp	specific heat capacity, kJ $kmol^{-1}$ K^{-1}
De	effective diffusivity, $m^2 s^{-1}$
Dim	diffusivity of component i in the gas mixture, $m^2 s^{-1}$
Dp	particle diameter, m
Ei	activation energy for i*th* reaction, kJ $kmol^{-1}$
F	volume force vector, kg m^{-2} s^{-2}
Ke1	equilibrium constant, MPa^3
u	velocity vector, m s^{-1}
ur	radial velocity, m s^{-1}
uz	axial velocity, m s^{-1}
yi	mole fraction for ith component in gas phase, -
T	viscous stress tensor, Pa
κ	permeability of porous media, Pa

Greek letters

ρ_B	reactor bulk density, kg m^{-3}
φ_s	sphericity, -
ϑ_c	critical volume, cm^3 $kmol^{-1}$

1. INTRODUCTION

Gasoline is a very widely used product of petroleum refineries that plays an important role in our modern life. Increasing demand on this product motivated researchers to search for processes to convert other fractions of petroleum to gasoline. Catalytic naphtha reforming is one of the most widespread processes used for this purpose. In this process, naphtha, that is a mixture of hydrocarbons in $c_5 - c_{12}$ range, converts to high-octane number gasoline called reformate.

Improving of naphtha reforming process efficiency is a very important field study and

has been investigated extensively. Liu et al. [1] and Vicerich et al. [2] modified the catalyst of catalytic naphtha reforming process and thus enhancing the process yield. Weifeng et al. [3], Hongjun et al. [4], and Mahdavian [5] studied the application of continuous catalytic configuration in naphtha reforming process. By applying this process, the catalyst activity increases and more reformate with higher aromatic content produces. Rahimpour et al. [6] suggested a fluidized membrane reactor for naphtha reforming. In this configuration, hydrogen penetrates through membrane and according to thermodynamic equilibrium, the reaction products increase.

Pressure drop contribute to decrease in reaction rate and yield, as well as operational problems. Thus, many researchers have been focused on finding a remedy for this serious problem in reactors. One of the suggested configurations for reducing the pressure drop is radial flow spherical packed-bed reactor (RF–SPBR), in which the space between the two concentric spheres is filled by catalyst. Rahimpour et al. [7] investigated the application of this reactor setup for naphtha reforming, and concluded that spherical reactor could be replaced by the conventional tubular reactor. They also studied a novel combination of spherical and membrane tubular reactors of the catalytic naphtha reforming process [8].

Another reactor setup, purposed for pressure drop reduction, is axial flow spherical packed–bed reactor (AF–SPBR). The AF–SPBR operates better than AF–TPBR due to lower pressure drop, that contribute to higher input molar flow rate or lower required surface, lower power supply of recompression, and also lower material thickness requirement. It is also superior to RF–SPBR because of better feed distribution, easier application of membrane technology, and etc. [9, 10].

Computational Fluid Dynamics (CFD) is a powerful and very widely used tool for modeling and optimization of reactors and other process vessels. Many researchers applied this method in their studies. For instance, Toit et al. [11] presented a systems CFD model of a packed bed high temperature gas-cooled nuclear reactor. Gao et al. [12] developed a 3D CFD model based on the Eulerian–Eulerian approach to describe the steady-state liquid–solid two-phase flow in the tubular loop propylene polymerization reactor. Fazeli et al. [13] modeled hydrogen production in a zigzag and straight catalytic wall coated micro channel reactor by CFD method. Kareeri et al. [14] investigated the flow distribution in four possible configurations of a radial flow reactor using Computational Fluid Dynamics. Other investigators also used this method in different reactor configurations and for different purposes [15-20].

Although a more complex modeling is not necessarily the better one, the simplicity of the modeling should not reduce the predictive capability of the presented model. One of the parameters, which affect on the complexity of the modeling, is choosing spatial variable that is the basis of writing the mass, energy, and momentum balances. In the previous work [9], a homogeneous one-dimensional (1-D) model has been considered for naphtha reforming process in an AF-SPBR. In this study, CFD model has been used to develop a homogeneous two-dimensional (2-D) model for this reactor setup. Obtained data from 2D analyses has been compared with 1D model to find out the differences between them.

2. REACTION SCHEME AND KINETIC

The kinetic reactions that were presented by Smith are used in this paper. In this model, the catalytic naphtha reforming reaction is categorized into four dominant reactions, including:

1. 1) Dehydrogenation of naphthenes to aromatics.
   $Naphthenes(C_nH_{2n}) \longleftrightarrow Aromatics(C_nH_{2n-6})+3H_2$
2. 2) Dehydrocyclization of paraffins to naphthenes.
   $Naphthenes(C_nH_{2n}) + H_2 \longleftrightarrow Paraffins(C_nH_{2n+2})$
3. 3) Hydrocracking of naphthenes to lower hydrocarbons.
   $Naphthenes(C_nH_{2n})+ n/3H_2 \longrightarrow Lighter\ ends(C_1\text{-}C_5)$
4. 4) Hydrocracking of paraffins to lower hydrocarbons.
   $Paraffins(C_nH_{2n+2})+(n-3)/3H_2 \longrightarrow Lighter\ ends(C_1\text{-}C_5)$

These reactions are described with following rate experitions:

$$r_1 = \left(\frac{k_{f1}}{K_{e1}}\right)\left(k_{e1}p_n - p_a p_h^3\right) \quad (1)$$

$$r_2 = \left(\frac{k_{f2}}{K_{e2}}\right)\left(k_{e2}p_n p_h - p_p\right) \quad (2)$$

$$r_3 = \left(\frac{k_{f3}}{p_t}\right)p_n \quad (3)$$

$$r_4 = \left(\frac{k_{f4}}{p_t}\right)p_p \quad (4)$$

,where k_{fi} and k_{ei} are forward rater constant and equilibrium constant, respectively.

3. PROCESS DESCRIPTION

3.1. CONVENTIONAL PROCESS

Naphtha reforming is a major process practiced extensively by petroleum refineries and the petrochemical industry in order to convert paraffins and naphthenes into aromatic. A simplified process flow diagram for catalytic reforming is depicted in Fig. 1.

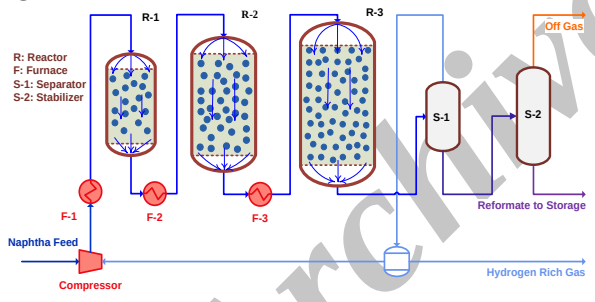

Fig. 1
A simplified process flow diagram for catalytic reforming

3.2.SPHERICAL REACTOR SETUP

Due to the drawbacks of tubular packed bed reactor such as pressure drop, high manufacturing costs, and low production capacity, the application of spherical packed bed reactor with axial flow has been suggested. Total reactor volume should not be filled with catalyst because the cross sectional area of the reactor is smaller near the inlet and outlet and the presence of catalyst in these areas would cause substantial pressure drop. Thus, two screens are placed near the reactor entrance and exit to hold the catalyst. A more detailed schematic of spherical reactor is drawn in fig 2. The presence of radial and axial flow distribution is shown obviously in this figure.

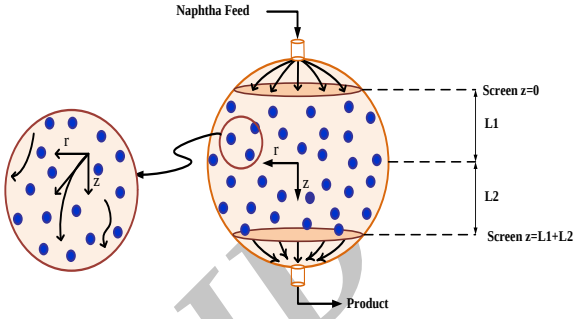

Fig.2
Schematic of flow in spherical reactor

4. REACTOR MODELING

In the previous study [9], one dimensional (axial direction) model of AF–SPBR for naphtha reforming process has been established. In this work, a homogeneous model in both axial and radial direction for an AF–SPBR has been presented. In this modeling, heat and mass balance equations are coupled with the kinetic relations and other auxiliary correlations,and then solved with CFD software.

The energy and mass balance equations are expressed as follow:

$$K_{eff}\frac{1}{A_c}\frac{\partial}{\partial z}\left(A_c\frac{\partial T}{\partial z}\right)+K_{eff}\frac{1}{r^2}\frac{\partial}{\partial r}\left(r^2\frac{\partial T}{\partial r}\right)-\frac{1}{A_c}\frac{\partial}{\partial z}\left(\rho A_c u_z c_p\left(T-T_{ref}\right)\right)$$
$$-\frac{1}{r^2}\frac{\partial}{\partial r}\left(\rho r^2 u_r c_p\left(T-T_{ref}\right)\right)+\rho_B a\sum_{i=1}^{m}\Delta H_i r_i=\varepsilon\frac{\partial\left(\rho c_p\left(T-T_{ref}\right)\right)}{\partial t} \quad (5)$$

$$D_{ej}\frac{1}{A_c}\frac{\partial}{\partial z}\left(A_c\frac{\partial C_i}{\partial z}\right)+D_{ej}\frac{1}{r^2}\frac{\partial}{\partial r}\left(r^2\frac{\partial C_i}{\partial r}\right)-\frac{1}{A_c}\frac{\partial}{\partial z}\left(A_c u_z C_j\right)-\frac{1}{r^2}\frac{\partial}{\partial r}\left(r^2 u_r C_j\right)$$
$$+\rho_B a\sum_{\substack{i=1\\ j=1,2,\ldots,n}}^{m}\vartheta_{ij}r_i=\varepsilon\frac{\partial C_j}{\partial t} \quad (6)$$

,where K_{eff} is the thermal conductivity of the gas phase; A_c the cross section area; T the temperature; ρ the density of gas phase; c_p the heat capacity of gas phase; a the catalyst

activity; ΔH the heat of reaction; ϵ the void fraction; r_i the reaction rate; D_{ej} the effective diffusiviy of component j; C the gas phase concentration; ρ_B the catalyst bulk dencity; v_{ij} the stoichiometry coefficient of the reactant j in the reaction i.
The momentum balance is obtained from a combination of the Navier-Stokes and the Brinkman equations:

Navier-Stokes equation:

$$\rho\frac{\partial u}{\partial t}+\rho(u.\nabla)u=\nabla.\left[-pI+\tau\right]+F \quad (7)$$

Brinkman equation:

$$\frac{\rho}{\varepsilon_p}\frac{\partial u}{\partial t}+\left(\frac{\mu}{\kappa}+Q\right)u=\nabla.\left[-pI+\frac{1}{\varepsilon_p}\left\{\mu(\nabla u+(\nabla u)^T)-\frac{2}{3}\mu(\nabla.u)I\right\}\right]+F \quad (8)$$

,where u is the velocity vector; τ the viscous stress tensor; F the volume force vector; ε_p the porosity; κ the permeability of the porous medium; Q the mass source or mass sink; μ the fluid viscosity.
the boundary and initial conditions are written as:

$$z=z_0: C_j=C_{j0}, T=T_0, u_z=u_{z_0},\ u_r=0 \quad (9)$$

$$z=l:\ \frac{\partial C_j}{\partial z}=0,\ \frac{\partial T}{\partial z}=0, \frac{\partial u_z}{\partial z}=0,\ u_r=0 \quad (10)$$

$$r=R:\ \frac{\partial C_j}{\partial r}=0,\ \frac{\partial T}{\partial r}=0,\ \frac{\partial u_r}{\partial r}=0 \quad (11)$$

$$r=0:\ \frac{\partial C_j}{\partial r}=0,\ \frac{\partial T}{\partial r}=0,\ \frac{\partial u_r}{\partial r}=0 \quad (12)$$

The pressure drop across the catalytic bed is expressed by Ergun equation. Viscous losses and kinetic energy losses have been considered in this equation. This equation for axial and radial directions derived as bellow:
Axial direction:

$$\frac{dp}{dz}=\frac{150\mu(1-\varepsilon)^2}{\varphi_s^2 d_p^2\varepsilon^3}u_z+\frac{1.75\rho(1-\varepsilon)}{\varphi_s d_p\varepsilon^3}u_z{}^2 \quad (13)$$

Radial direction:

$$\frac{dp}{dr}=\frac{150\mu(1-\varepsilon)^2}{\varphi_s^2 d_d^2\varepsilon^3}u_r+\frac{1.75\rho(1-\varepsilon)}{\varphi_s d_p\varepsilon^3}u_r{}^2 \quad (14)$$

,where dP is the pressure gradient; d_p the particle diameter; φ_s the Sphericity (which is unity for spherical particles); ρ the fluid density. It should be mentioned that $uz=Q/Ac$ and $ur=Q/A$, in which Q is the volumetric flow rate.

5. MODEL VALIDATION

In order to investigate the accurecy of the present model, the modeling results of tubular packed bed reactor (TPBR), 1-D spherical packed bed reactor (SPBR), and 2-D spherical packed bed reactor (SPBR) are compared with plant data. Coresponding results are presented in table 1. As obvious, the plant data and simulation results are in good agreement that shows the accuracy of the suggested model.

Table 1. Comparison of models with the plant data

Reactor number	Aromatic in reformate (mole %)			
	plant	TPBR	SPBR	
			1D	2D
1	-	32.59	33.38	33.13
2	-	44.95	45.17	45.82
3	57.7	54.74	54.53	53.46

Inlet temperature (K)		Outlet temperature (K)			
	plant	plant	TPBR	SPBR	
				1D	2D
1	777	722	728.10	724.25	726.60
2	777	753	746.15	747.01	751.18
3	775	770	771.24	770.16	769.57

6. RESULTS AND DISCUSSION

In the AF–SPBR, the feedstock stream is entered axially and moves in both axial and radial directions through the reactor. Although eliminating the movement of the fluid in the radial direction would increase the simplicity of the modeling, but it may also decrease the accuracy of the obtained results. Thus, the importance and the effect of considering two-dimensional distributions in the modeling of the spherical packed-bed reactor should be evaluate.

In order to investigate the differences between 1D and 2D model of AF-SPBR, the obtained velocity, temperature, and concentration distribution of both models are compared. It should be mentioned that this comparison is made over the first reactor and the entrance velocity is assumed to be 0.47 m/s.

2D velocity distribution is depicted in fig. 3. It is observed from this figure that the velocity in the input and output of the reactor is in axial direction, and in distances far from the center of the reactor, radial velocity appears too. In a cross sectional element near the center of the reactor, axial distribution of velocity is dominated, because by increasing the ratio of the inlet cross section radius over the length of the reactor, the velocity distribution approaches to 1D velocity in the axial direction and the effect of the radial direction could be neglected.

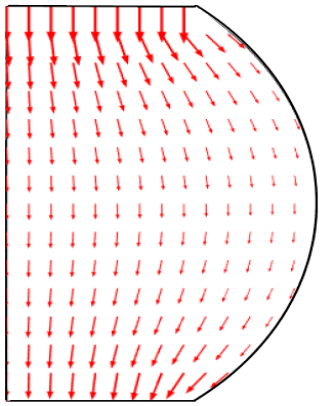

Fig. 3
2D velocity distribution in the first spherical packed bed reactor

Fig. 4(a) shows the 1D and 2D naphthene concentration distribution in the central cross section area of the first reactor. In 1D distribution, the change of concentration in axial direction is taken into account and since this diagram is drawn in a specific length, no change is observed with increase in radius. But in 2D distribution, radial change is taken into account too, and obviously the naphthene concentration decreases with increasing of the radius. This reduction is steeper near the wall of the reactor that is because of the increase in residence time and consequently increment in naphthene consumption.

Aromatic concentration in the central cross section area is depicted in fig. 4(b). Similar to naphthene, aromatic concentration remains constant in 1D distribution, but in 2D distribution it increase with radius. Temperature variation with radius in the central cross section area is illustrated in fig. 4(c). Like other parameters, the temperature profile is a straight line in 1D distribution. However, in 2D distribution, temperature falls with radius because of endothermic naphtha reforming reaction.

In fig. 5(a), 1D and 2D naphthene average concentration distribution through the length of the first reactor is depicted. Naphthene consumes in the naphtha reforming reaction, therefore it's concentration decreases. Although 1D and 2D naphthene concentration distributions are differ slightly from each other, but this difference in the output of the

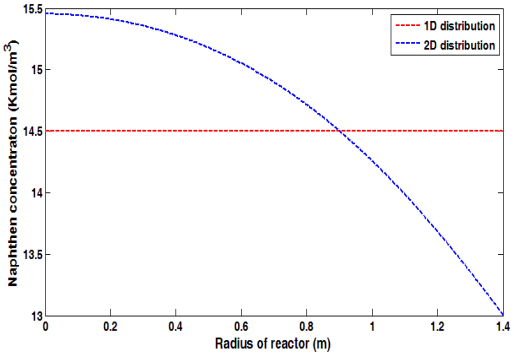

(a)

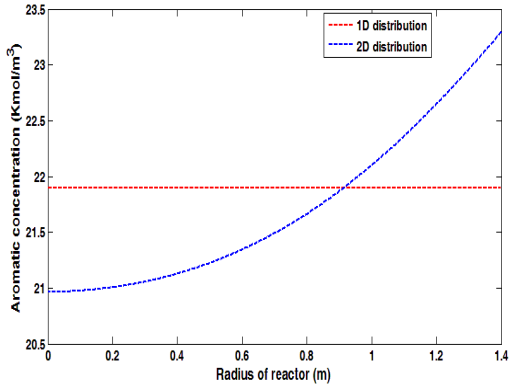

(b)

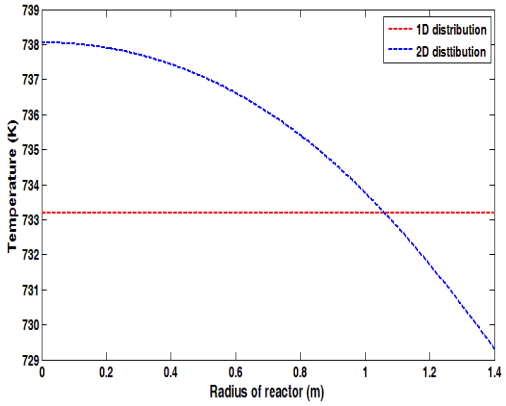

(c)

Fig. 4 (a) Comparison of 1D and 2D distribution of (a) naphthene concentration (b) aromatic concentration (c) temperature in the central cross section area in the first reactor

reactor is only 1.72%, that is not considerable. This case is also observed in 1D and 2D aromatic average concentration and average temperature distribution that are shown in fig. 5(b) and (c), respectively. The difference between 1D and 2D analyse of aromatic average concentration and average temperature in the output of the reactor is 0.86% and 0.32%, respectively.

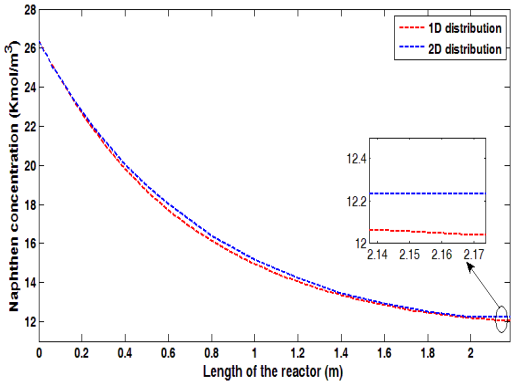

(a)

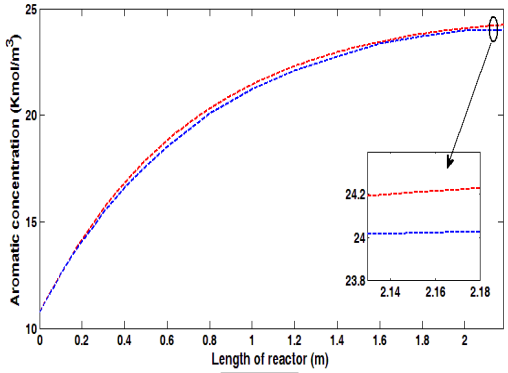

(b)

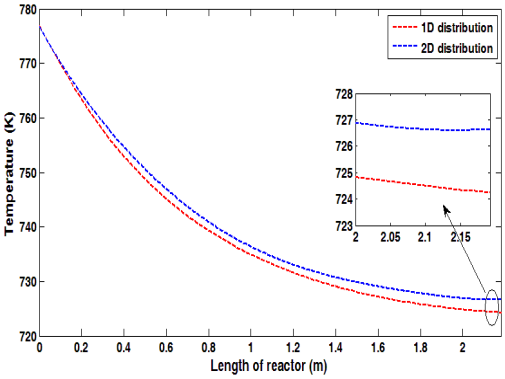

(c)

Fig. 5. Comparison of 1D and 2D distribution of **(a)** naphthene average concentration **(b)** aromatic average concentration **(c)** average temperature through the length of the first reactor distribution of aromatic average

To present an overall outlook on the difference between 1D and 2D concentration distribution, 1D and 2D naphthene concentration distribution in the first reactor is revealed in fig. 6. The effect of considering radial changes of naphthene concentration in 2D distribution respect to 1D distribution is obviously observed via comparing the change of color in fig. 6(a) and (b). In 2D reactor modeling, naphthene consumption is considered in both axial and radial directions, therefore, more naphthene is converted to aromatics compared to the 1D modeling.

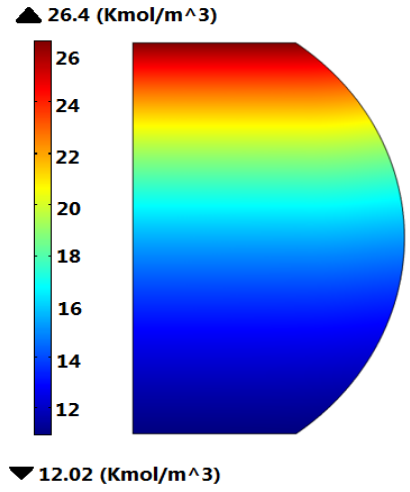

(a)

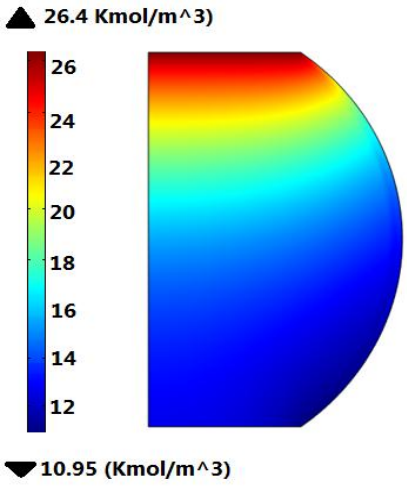

(b)

Fig.6
(a) 1D naphthene concentration in naphtha reforming spherical packed bed reactor. (b) 2D naphthene concentration in naphtha reforming spherical packed bed reactor.

7. CONCLUSION

Presenting an appropriate model for catalytic naphtha reforming process could be very useful due to the industrial importance of this process. Previously, One-dimensional model of AF-SPBR for naphtha reforming reaction has been presented [9], in which only axial variations of velocity, concentration, and temperature were considered. In order to take into account the parameter changes in radial direction as well as axial one, a 2D model was presented in this work. After writing the related equations and relations, CFD software was used to present a homogeneous 2D model for this reactor setup, and obtained data were compared with 1D model.

The effect of considering radial direction on the velocity profile was considerable near the wall of the reactor and in distances far from the center of the reactor. The change of naphthene and aromatic concentration and temperature with radius in 2D model was also more noticeable near the wall of the reactor due to the increase in the reduction time. The change of naphthene and aromatic average concentration and average temperature with the length of the reactor in 2D modeling was compared with 1D modeling results. The calculated differences were 1.72%, 0.86%, and 0.32% for naphthene and aromatic average concentration, and average temperature in the output of the reactor, respectively. Because of negligible difference between 1D and 2D modeling of AF-SPBR, 1D model could be used for prediction of the existing situation.

Keywords: catalytic naphtha reforming, axial flow, spherical packed-bed reactor, Computational Fluid Dynamic, two-dimensional modeling.

REFERENCES:

1. Liu, C., Qing Zhu, Wu, Z., Zhou, Z., Bhargava, G., Parasher, S., Rueter, M., Zhou, B., Chen, J.G., 2010, Increase of reformate yield by using polyacrylic acid as template in preparation of Pt/Re naphtha reforming catalysts, Appl. Catal. , A 390, pp. 19–25.
2. Vicerich, M.A., Especel, C., Benitez, V.M., Epron, F., Pieck, C.L., 2011, Influence of gallium on the properties of Pt–Re/Al2O3 naphtha reforming catalysts, Appl. Catal., A **407**, pp. 49-55.
3. Hou, W., Hu, Y., Su, H., J. Chu, 2004, Simulation, Sensitivity Analysis and Optimization of a Continuous Catalytic Reforming-Process, Proceedings of the 5Ih World Congress on Intelligent Control and Automation, June 15-19, Hangzhou, P.R. China.

4. Hongjun, Z., Mingliang, S., Huixin, W., Zeji, L., Hongbo, J., 2010, Modeling and Simulation of Moving Bed Reactor for Catalytic Naphtha Reforming, Pet. Sci. Technol. **28**, pp. 667-676.
5. Mahdavian, M., Fatemi, S., Fazeli, A., 2010, Modeling and simulation of industrial continuous naphtha catalytic reformer accompanied with delumping the naphtha feed, Int. J. Chem. React. Eng. **8**, Article A8.
6. Rahimpour, M.R., 2009, Enhancement of hydrogen production in a novel fluidized-bed membrane reactor for naphtha reforming, Int. J. hydrogen energy **34**, pp. 2235-2251.
7. Rahimpour, M.R., Iranshahi, D., Bahmanpour, A.M., 2010, Dynamic optimization of a multi-stage spherical, radial flow reactor for the naphtha reforming process in the presence of catalyst deactivation using differential evolution (DE) method, Int. J. hydrogen energy **35**, pp. 7498-7511.
8. M.R. Rahimpour, D. Iranshahi, E. Pourazadi, A.M. Bahmanpour, 2011, A comparative study on a novel combination of spherical and membrane tubular reactors of the catalytic naphtha reforming process Int. J. hydrogen energy **36**, pp. 505-517.
9. D. Iranshahi, E. Pourazadi, K. Paymooni, A.M. Bahmanpour, M.R. Rahimpour, A. Shariati, 2010, Modeling of an axial flow, spherical packed-bed reactor for naphtha reforming process in the presence of the catalyst deactivation, Int. J. hydrogen energy **35**, pp. 12784-12799.
10. M.R. Rahimpour, D. Iranshahi, E. Pourazadi, K. Paymooni, A.M. Bahmanpour, 2011, The Aromatic Enhancement in the Axial-Flow Spherical Packed-Bed Membrane Naphtha Reformers in the Presence of Catalyst Deactivation, AIChE J. **57**, pp. 3182-3198.
11. C.G. du Toit, P.G. Rousseau, G.P. Greyvenstein, W.A. Landman, 2006, A systems CFD model of a packed bed high temperature gas-cooled nuclear reactor, Int. J. Therm. Sci. **45**, pp. 70–85.
12. X. Gao, D.Shi, X.Chen, Z.Luo, 2010, Three-dimensional CFD model of the temperature field for a pilot-plant tubular loop polymerization reactor, Powder Technol. **203**, pp. 574–590.
13. A. Fazeli, M. Behnam, 2010, Hydrogen production in a zigzag and straight catalytic wall coated micro channel reactor by CFD modeling, Int. J. hydrogen energy **35**, pp. 9496-9503.
14. A.A. Kareeri, H.D. Zughbi, H.H. Al-Ali, 2006, Simulation of Flow Distribution in Radial Flow Reactors, Ind. Eng. Chem. Res. **45**, pp. 2862-2874.
15. J.E. Duran, F. Taghipour, M. Mohseni, 2009, CFD modeling of mass transfer in annular reactors, Int. J. Heat and Mass Transfer **52**, pp. 5390–5401.
16. X. Chen, D. Shi, X. Gao, Z. Luo, 2011, A fundamental CFD study of the gas–solid flow field in fluidized bed polymerization reactors, Powder Technol. **205**, pp. 276–288.
17. Á. Frías-Ferrer, I. Tudela, O. Louisnard, V. Sáez, M.D. Esclapez, M.I. Díez-García, P. Bonete, J. González-García, 2011, Optimized design of an electrochemical filter-press reactor using CFD methods, Chem. Eng. J. **169**, pp. 270–281.
18. X. Wanga, X. Jia , J. Wen, 2011, Transient CFD modeling of toluene waste gas biodegradation in a gas–liquid–solid three-phase airlift loop reactor by immobilized Pseudomonas putida, Chemical Engineering Journal **172**, pp. 735– 745.
19. Hekmat, A., Ebadi Amooghin, A., Keshavarz Moraveji, M., 2010, CFD simulation of gas–liquid flow behaviour in an air-lift reactor: determination of the optimum distance of the draft tube, Simul. Model. Pract. Theory **18**, pp. 927–945.
20. Simck, M., Mota, M., Ruzick, M.C., A.Vicente , Teixeira, J., 2011, CFD simulation and experimental measurement of gas holdup and liquid interstitial velocity in internal loop airlift reactor, Chem. Eng. Sci. **66**, pp. 3268–3279.
21. Iranshahi, D., Rahimpour, M.R., Asgari, A., 2010, A novel dynamic radial-flow, spherical-bed reactor concept for naphtha reforming in the presence of catalyst deactivation, Int. J. hydrogen energy **35** () 6261-6275.